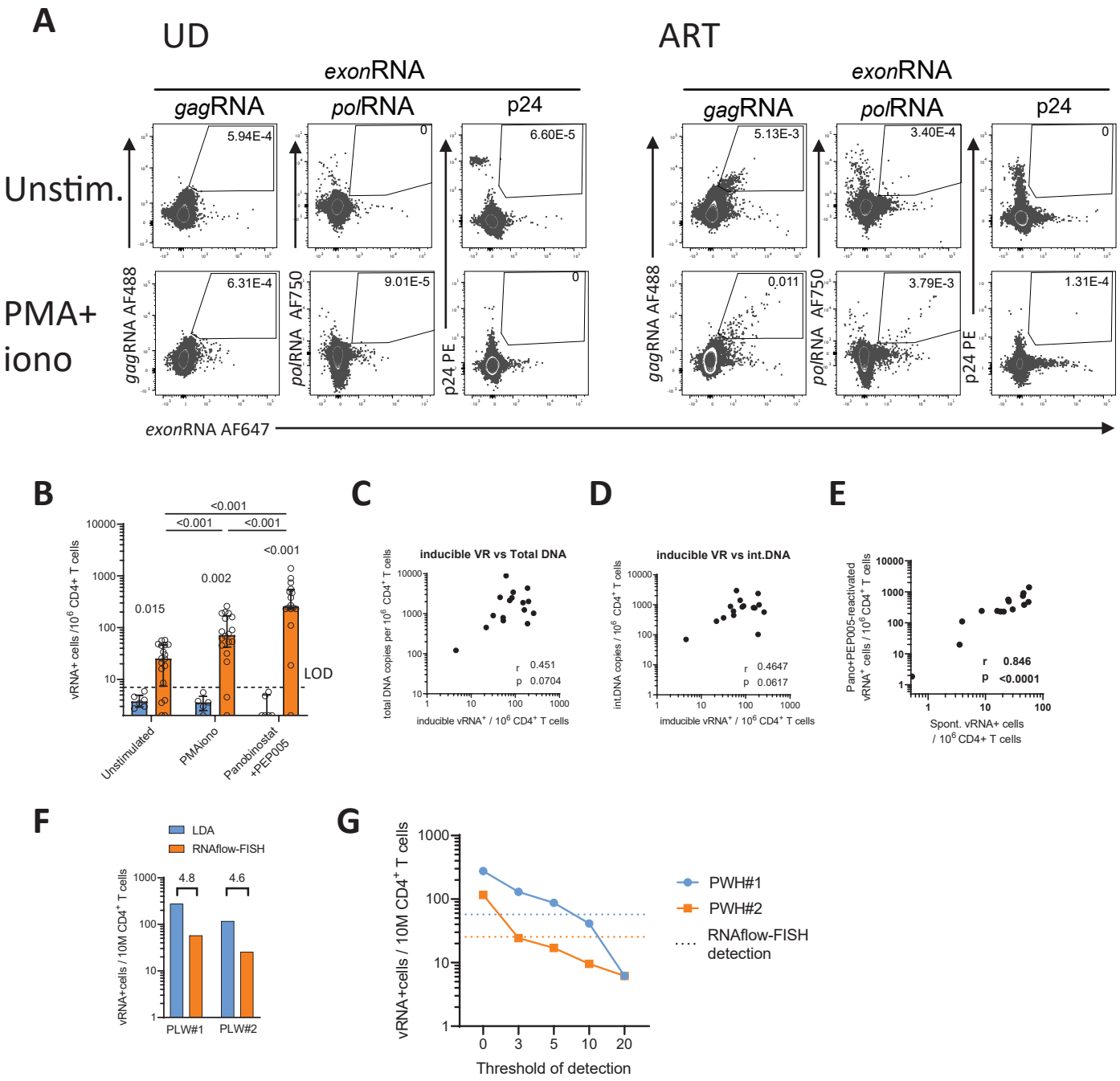

Supplemental Figure 1: Detection of vRNA expression in purified CD4+ T cells from participants on ART. Related to Figure 1.

Figure S1: Detection of vRNA expression in purified CD4$^+$ T cells from participants on ART. Related to Figure 1. (A) Gating strategy identifying vRNA$^+$ cells. (**B**) Complete quantification of vRNA$^+$ cells from UD and ART participants, i) without stimulation or ii) stimulated with PMAionomycin or iii) a combination of Panobinostat and Ingenol. Two statistical tests are shown: Mann-Whitney to cohort comparisons and Wilcoxon to compare unstimulated vs. PMAionomycin induction. The bars indicate the median, and the error bars illustrate the interquartile range. (**C-E**) Correlations between (**C**) total DNA vs. PMAionomycin-induced, (**D**) integrated DNA vs. PMAionomycin-induced, and (**E**) Panobinostat+Ingenol-induced vs. spontaneously active reservoir. R and p values from Spearman tests are indicated. N =18. (**F**) Compared quantifications of vRNA+ cells using a limiting dilution RT-qPCR assay and the HIV RNAflow-FISH assay in two PWH. (**G**) Quantification of the RT-qPCR with different threshold of detection. The dash bar correspond to paired HIV RNAflow-FISH detection. The error bars represent standard deviation of 11 technical replicates.

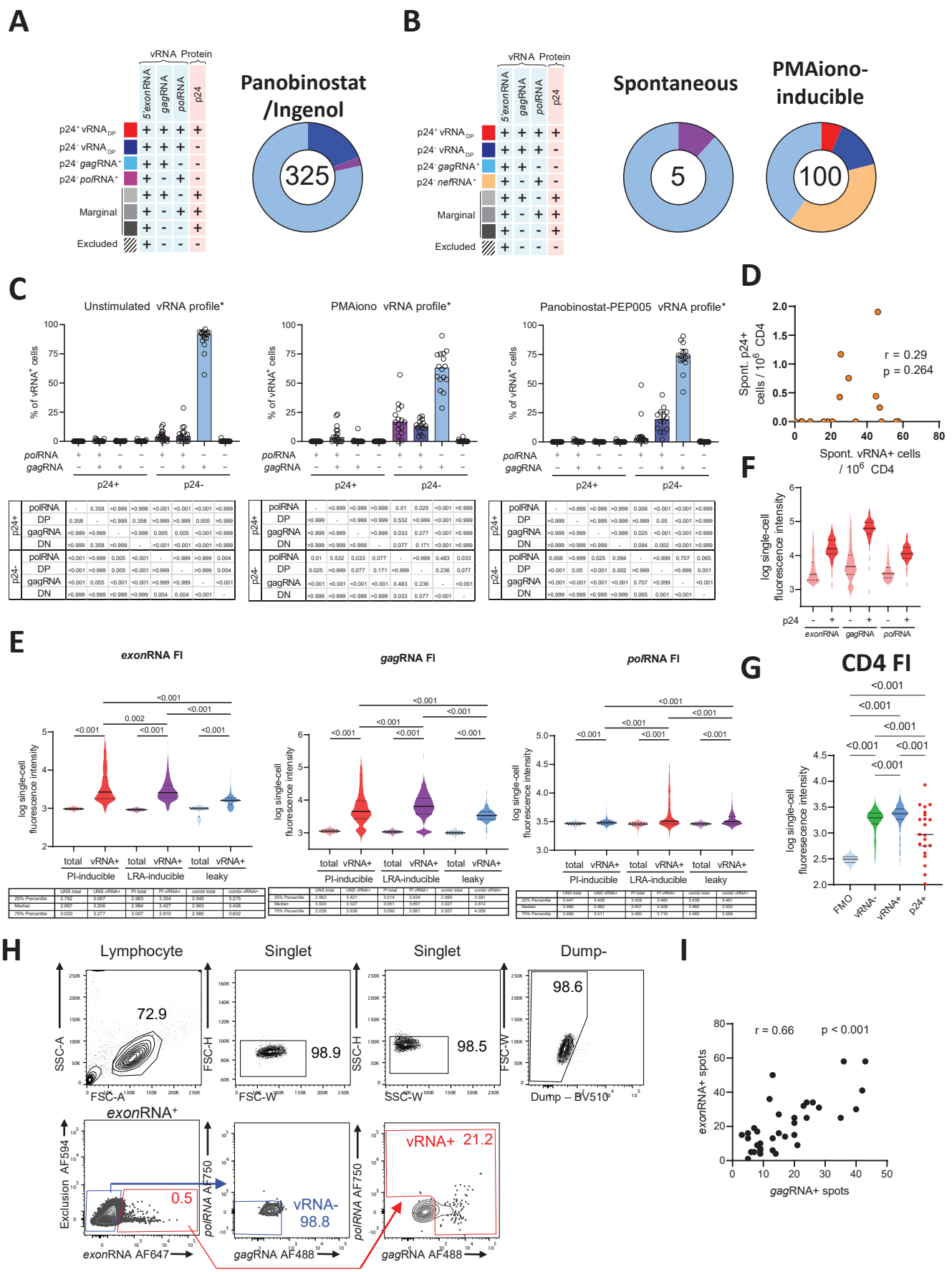

Supplemental Figure 2: Details of the viral gene expression in vRNA+ cells. Related to Figure 2.

Figure S2: Details of the viral gene expression in vRNA+ cells. Related to Figure 2. (**A**) A legend listing the different theoretical vRNA+ populations defined by *exon*RNA, *gag*RNA, and *pol*RNA probesets is shown on the left. Donut charts presenting the median proportions of each vRNA+ subpopulation for the combinatory Panobinostat+Ingenol stimulation are shown on the right. (**B**) Legend listing the different theoretical vRNA+ populations using *exon*RNA, *gag*RNA, and *nef*RNA probesets. Donut charts presenting the median proportions of each vRNA+ subpopulation for the spontaneously active or PMAionomycin-induced reservoirs. In **AB**, the numbers in the donut hole represent the median $vRNA^+$ cells per 10^6 CD4 T cells. (**C**) The histograms report the proportions of each $vRNA^+$ subpopulation for spontaneously active, PMAionomycin, or Panobinostat+Ingenol-induced reservoirs, supporting Figures 2D and S2A. The bars represent median values. All results from a Friedman test are shown underneath. (**D)** Correlations between spontaneously active $p24^+$ and $vRNA^+$ cells. R and p values are indicated. (**E**) Violin plots showing single-cell fluorescence intensities for all $vRNA^+$ cells detected in 17 participants, including Panobinostat+Ingenol stimulation. (**F**) Single-cell fluorescence intensities of *exon*RNA, *gag*RNA and *pol*RNA in translation-competent $vRNA^+p24^+$ cells upon induction by PMAionomycin. For the sake of comparison, the total $vRNA^+$ population is also represented. N=17. (**G**) Violin plots showing single-cell CD4 fluorescence intensities in $vRNA^+$ versus $vRNA^-$ cells, without stimulation. FMO levels are also indicated. The results from Wilcoxon tests are shown above. N=17 (1 participant with no active vRNA was excluded to maintain a side-by-side comparison). (**H**) Gating strategy for $vRNA^-$ and vRNA+ cell sorting, prior to study by confocal fluorescence microscopy. (**I**) Correlation between the number of *exon*RNA^+ and *gag*RNA^+ spots per cell.

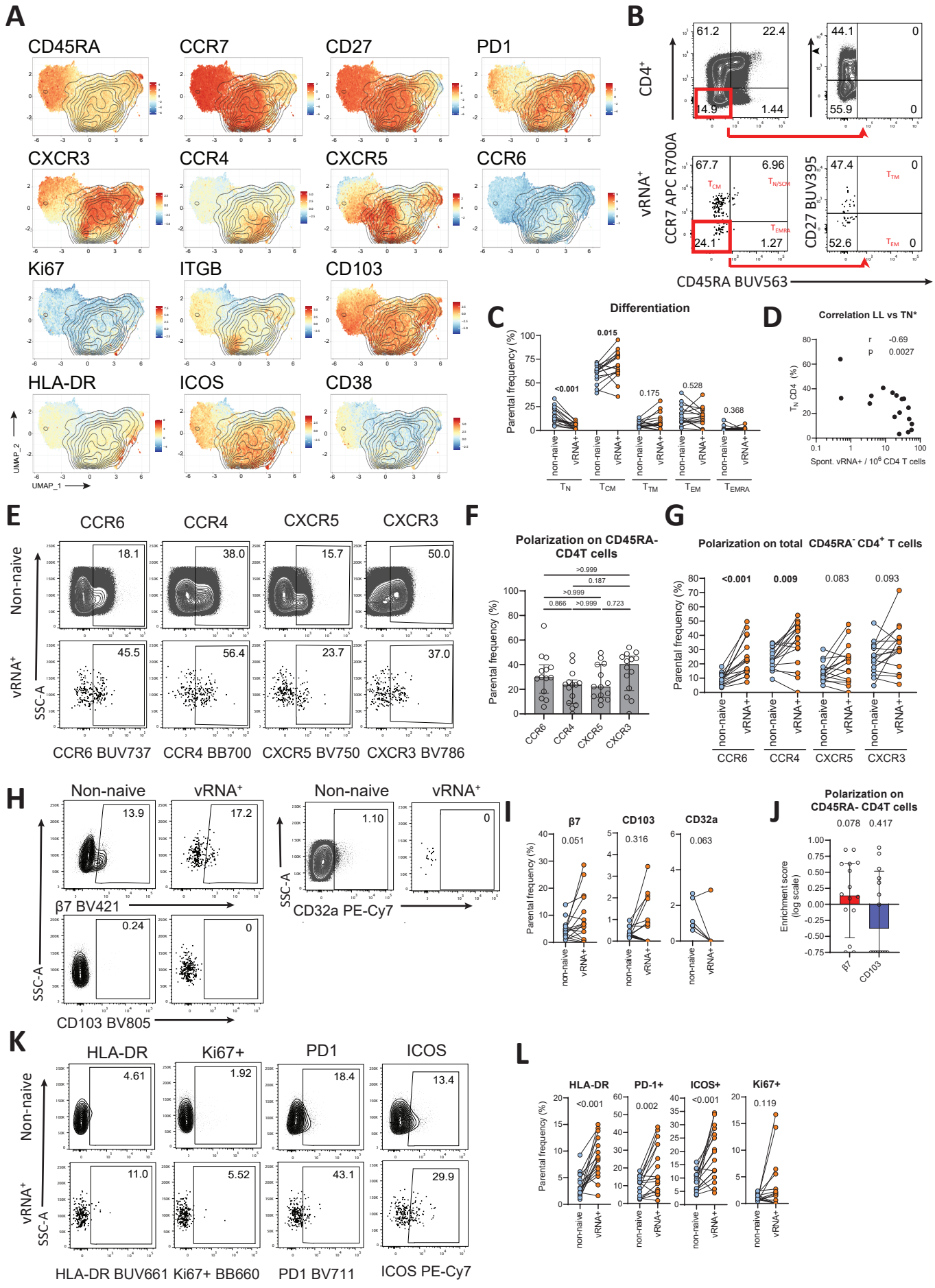

Supplemental Figure 3: Phenotyping of spontaneously active reservoirs. Related to Figure 3.

Figure S3: Phenotyping of spontaneously active reservoirs. Related to Figure 3. (**A**) Multiple iterations of the UMAP representation from Figure 3 where the expression level of each loaded parameter was individually layered. Warm colors indicate high expression, and cold colors are for lower expression. Each feature was subject to scaling to ease the comparison. (**BC**) Univariate $CD4^+$ T memory analysis. (**B**) Representative gating strategy. (**C**) Relative enrichment of $vRNA^+$ cells compared to the parental CD4 T cell population. The enrichment is shown for the indicated CD4 T memory subsets, including T naïve. Wilcoxon tests are shown above. (**D**) Correlation between total $CD4^+$ T_N and active vRNA+ cells. N=17. (**EFG**) Univariate analyses of $vRNA^+$ cell polarization. (**E**) Representative gating strategy. (**F**) Median frequencies of each single total HIV-specific $CD45RA^-$ $CD4^+$ T cell polarization. The bars represent the median and the error bars, the interquartile range. (**G**) Relative enrichment of $vRNA^+$ cells compared to the parental $CD4^+$ T cell population for each tested polarization marker. Wilcoxon tests are shown above. (**HIJ**) Univariate analyses of β7 and CD103 expression on $vRNA^+$ cells. (**H**) Representative gating strategy. (**I**) Relative enrichment of $vRNA^+$ cells compared to the parental $CD4^+$ T cell population for each tested marker. Wilcoxon tests are shown above. (**J**) Enrichment score. (**KL**) Univariate analyses of activation markers on $vRNA^+$ cells. (**K**) Representative gating strategy. (**L**) Relative enrichment of $vRNA^+$ cells compared to the parental $CD4^+$ T cell population for each tested activation marker. Wilcoxon tests are shown above. (**A-C, E-L**) N=16 (2 participants had <5 $vRNA^+$ cells, our threshold for phenotyping).

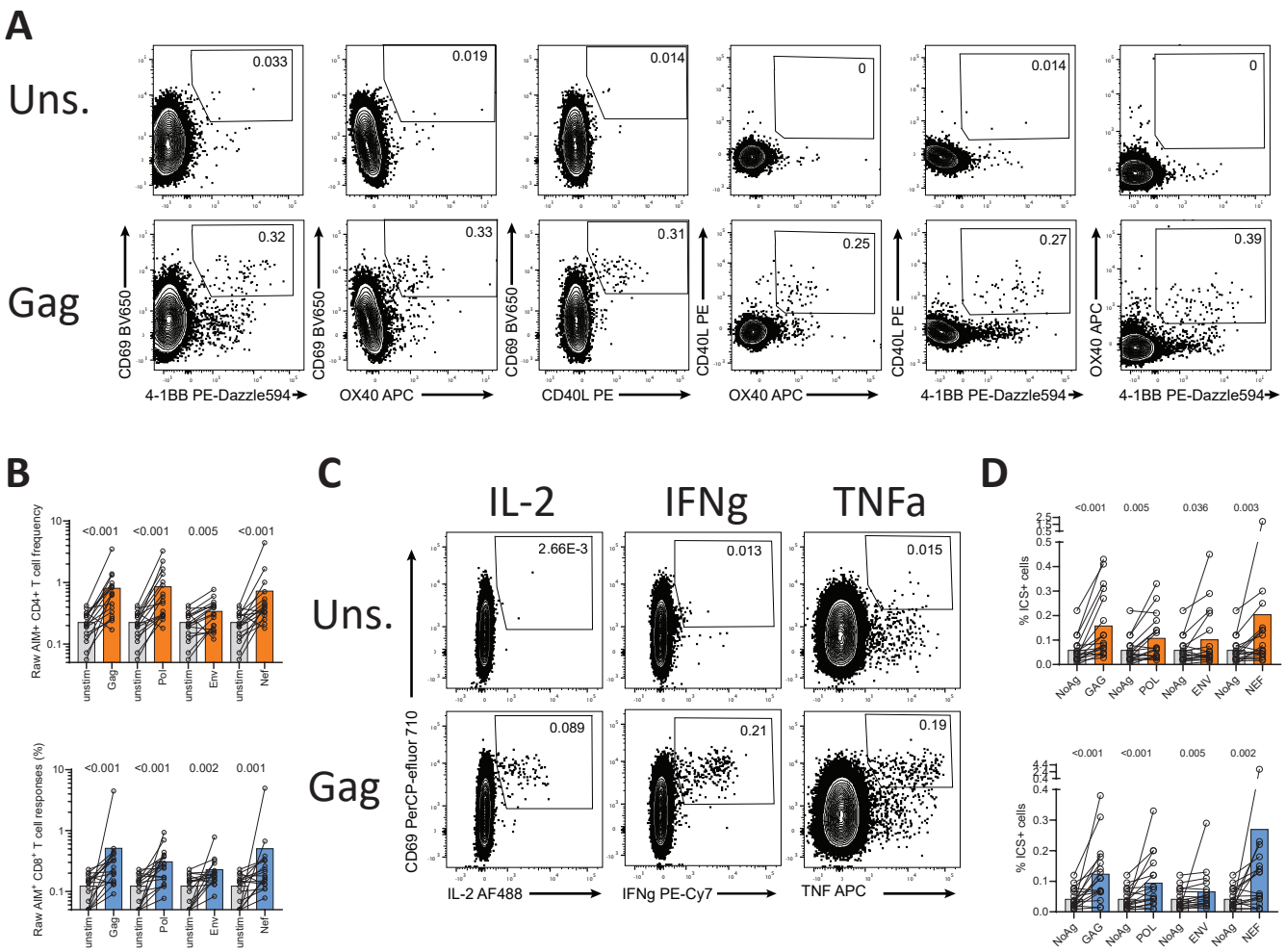

Supplemental Figure 4: AIM and ICS assays. Related to Figure 4.

Figure S4: AIM and ICS assays. Related to Figure 4. (**A**) Representative gating of each AIM pair was used for the ORgate analysis of Gag-specific $CD4^+$ T cell responses. The same gating was applied for Pol, Env, and Nef-specific $CD4^+$ T cells. (**B**) Raw $CD4^+$ (top) and $CD8^+$ (down) T cell responses, comparing the unstimulated vs. peptide-stimulated conditions. The bars indicate the median, and the error bars illustrate the interquartile range. The results from Wilcoxon tests are shown above the histograms. (**C**) Representative gating of each cytokine used for the ORgate analysis of Gag-specific effector $CD4^+$ T cell responses. The same gating was applied for Pol, Env, and Nef-specific $CD4^+$ T cells. (**D**) Raw $CD4^+$ (top) and $CD8^+$ (down) T cell responses compared the unstimulated vs. peptide-stimulated conditions. The bars indicate the median, and the error bars illustrate the interquartile range. The results from Wilcoxon tests are shown above the histograms. N=16 (1 participant had < 5 vRNA+ cells, therefore could not be phenotyped).

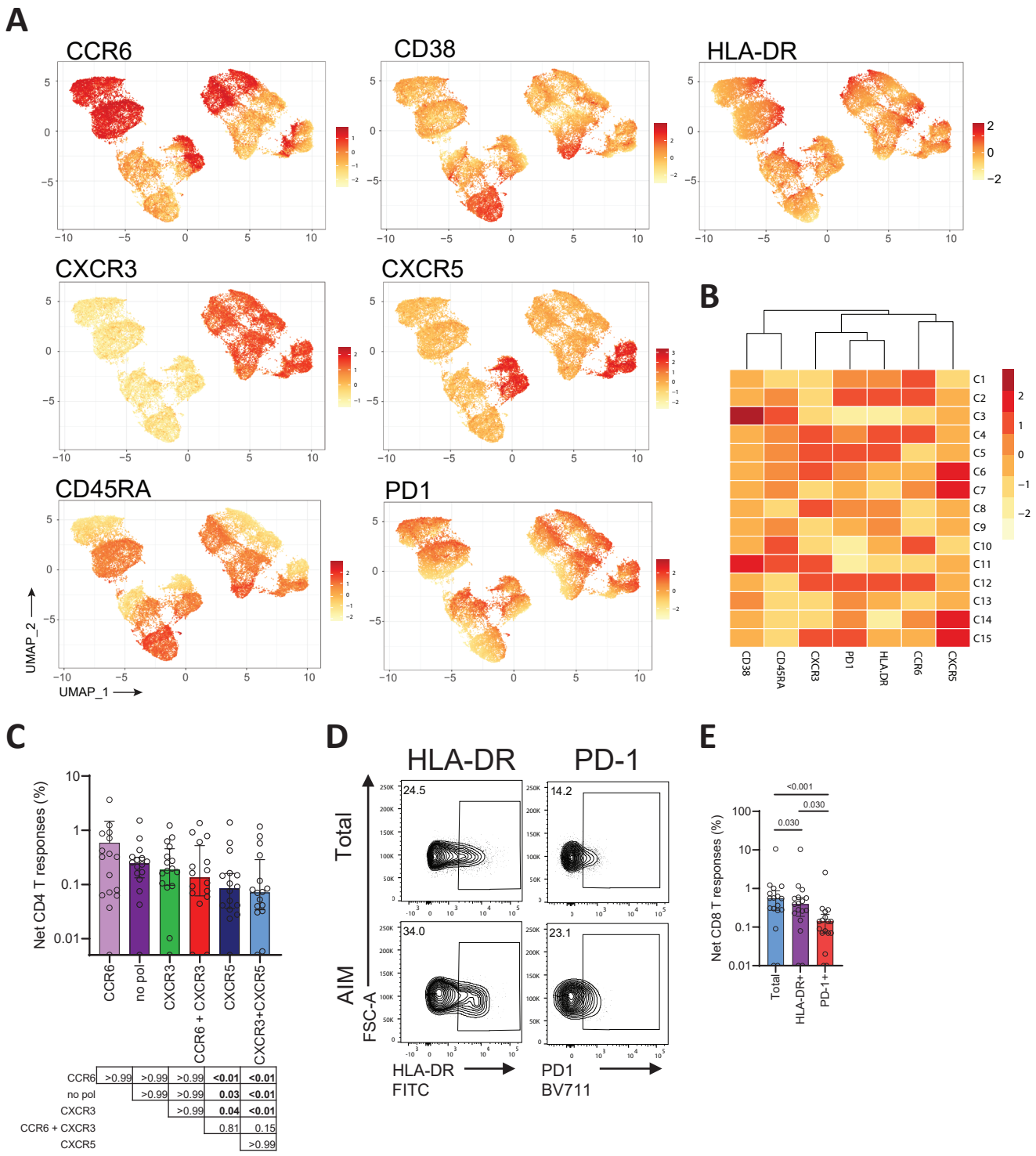

Supplemental Figure 5: Cell markers distribution in the AIM+ UMAP representation. Related to Figure 5.

Figure S5: Cell markers distribution in the AIM$^+$ UMAP representation. Related to Figure 5. (**A**) Multiple iterations of the same UMAP representation from Figure 6 where the expression level of each loaded parameter was individually layered. Warm colors indicate high expression, cold is for lower expression. Each feature was subject to scaling to ease comparison. (**B**) Heat map showing an unsupervised clustering of the 15 clusters defined by the MFI of each loaded parameter. N = 17. (**C**) Histogram showing the magnitudes of net HIV-specific AIM$^+$ CD4$^+$ T cell responses per superclusters. The bars indicate median values, and the error bars represent the interquartile range. Stats shown underneath are results for a Friedman test with multiple comparisons, with Dunn correction. N=17 (**D**) Representative examples of HLA-DR and PD1 AIM$^+$ CD8$^+$ T cell gatings. (**E**) Histogram showing the magnitudes of net HIV-specific AIM$^+$ CD8$^+$ T cell responses. The bars indicate median values, and the error bars represent the interquartile range. Stats shown underneath are results for a Friedman test with multiple comparisons, with Dunn correction. N=17

Table S1. Clinical characteristics of the study participants. Related to Figures 1 to 6. †

	PLWH on ART n = 18	Uninfected controls n = 6
Age (year old)	**55** (51-58)	**51** (42-56)
Sex	**100%** male	**50%** male **50%** female
Duration of infection (y)	**19.6** (12.9-24.1)	NA
Time before ART (y)	**3.9** (1.3-11.9)	NA
Time on ART (y)	**10.8** (6.6-26.9)	NA
CD4 counts	**619** (436-813)	**582** (531-703)
CD8 counts	**1179** (565-1373)	**298** (252-359)
CD4/CD8 ratio	**0.52** (0.34-1.15)	**2.14** (1.99-2.28)
Log Pre-ART VL	**4.41** (4.21-4.94)	-

† Values displayed in bold are medians. Interquartile ranges are shown in parentheses for continuous variables. Percentages were used for categorical variables.

Table S2. Flow cytometry antibody staining panel for viral reservoir characterization. Related to the STAR Methods section.

Marker-Fluorophore	Clone	Vendor	Catalog #
In culture			
CCR4 – BB700	1G1	BD Biosciences	566475
CCR7 – APC R700	2-L1-A	BD Biosciences	566767
CXCR5 – BV750	RF8B2	BD Biosciences	747111
CXCR3 – BV786	G025H7	BioLegend	353738
CCR6 – BUV737	11A9	BD Biosciences	564377
CD103 – BUV805	Ber-ACT8	BD Biosciences	748501
Surface staining			
CD4 – BB630	SK3	BD Biosciences	CUSTOM
CD38 – BB790	HIT2	BD Biosciences	CUSTOM
β7-integrin – BV421	Fib504	BD Biosciences	564283
CD8 – BV480	RPA-T8	BD Biosciences	566121
CD14 – BV480	M5E2	BD Biosciences	746304
CD16 – BV480	3G8	BD Biosciences	566108
CD19 – BV480	HIB19	BD Biosciences	746457
CD56 – BV480	NCAM16.2	BD Biosciences	566124
PD1 – BV711	EH12.2H7	BioLegend	329928
CD27 – BUV395	L128	BD Biosciences	563815
CD3 – BUV496	UCHT1	BD Biosciences	612941
CD45RA – BUV563	HI100	BD Biosciences	612926
HLA-DR – BUV661	G46-6	BD Biosciences	612980
ICOS – PE-Cy7	ISA-3	eBiosciences	25-9948-42
Intracellular staining			
p24 – PE	KC57	Beckman Coulter	6604667
Ki67 – BB660	B56	BD Biosciences	624295
RNAflow-FISH probeset			
*exon*RNA probe – AF647	NA	Thermofisher	VF1-6000978-210
*gag*RNA probe – AF488	NA	Thermofisher	VFKA3CY-210
*pol*RNA probe – AF750	NA	Thermofisher	VF6-18315
Dye			
LIVE/DEAD Fixable dead cell eFluor506	NA	Thermofisher	65-0866-14

Table S3. Flow cytometry antibody staining panel for activation-induced marker assay. Related to the STAR Methods section.

Marker-Fluorophore	Clone	Vendor	Catalog #
In culture			
CD183 (CXCR3) – BV605	G025H7	Biolegend	353728
CD185 (CXCR5) – BV421	J25D4	Biolegend	356920
CD196 (CCR6) – BUV737	11A9	BD	564377
Surface			
CD3 – BUV496	UCHT1	BD	612941
CD4 – BB630	SK3	BD	624294
CD8 – BV570	RPA-T8	Biolegend	301037
CD14 – BV480	M5E2	BD	746304
CD19 – BV480	HIB19	BD	746457
CD38 – BB790	HIT2	BD	CUSTOM
CD45RA – PerCP Cy5.5	HI100	BD	563429
CD69 – BV650	FN50	Biolegend	310934
CD134 (OX40) - APC	ACT35	BD	563473
CD137 (4-1BB) – PE-Dazzle 594	4B4-1	Biolegend	309826
CD154 (CD40L) - PE	TRAP1	BD	555700
CD279 (PD1) – BV711	EH122H	Biolegend	329928
HLA-DR - FITC	LN3	Biolegend	327005
Dye			
LIVE/DEAD Fixable dead cell	N/A	Thermo Fisher Scientific	L34960

Table S4. Flow cytometry antibody staining panel for intracellular detection. Related to the STAR Methods section.

Marker-Fluorophore	Clone	Vendor	Catalog #
Surface			
CD3 – BV650	UCHT1	BD Biosciences	563852
CD4 – BV605	RPA-T4	BD Biosciences	562658
CD8 – APCeFluor780	SK1	eBioscience	47-0087-42
CD14 – V500	M5E2	BD Biosciences	561391
CD19 – V500	H1B189	BD Biosciences	561121
CD69 – PerCP-eFluor710	FN50	eBioscience	46-0699-42
CD107A – BV785	H4A3	BD Biosciences	563869
PD-1 – BV421	EH12.2H7	Biolegend	329920
Intracellular			
IFN-γ – PE-Cy7	B27	BD Biosciences	557643
CD154 (CD40L) – PE	TRAP1	BD Biosciences	555700
IL-2 – AF488	MQ1-17H12	Biolegend	500314
TNF - APC	Mab11	BD Biosciences	562084
Dye			
Aquavivid	NA	Invitrogen	L34966

Table S5: Single-cell vRNA+ sequences accession numbers. Related to Figure 3.

Sequence number	GenBank accession number
PWH9_L3p1_A2_C0_434	OR105517
PWH5_L2p3_A9_PCR2_G9_C0_455	OR105518
PWH5_L2p2_F6_C0_290	OR105519
PWH5_L2p2_E10_C0_386	OR105520
PWH5_L2p2_E9_PCR2_E9_C0_454	OR105521
PWH5_L2p2_E3_C0_463	OR105522
PWH5_L2p2_D10_C0_432	OR105523
PWH5_L2p1_C12_PCR2_C12_C0_440	OR105524
PWH5_L2p1_C10_C0_473	OR105525
PWH5_L2p1_C6_PCR2_C6_C0_474	OR105526
PWH5_L2p1_B7_C0_325	OR105527
PWH5_L2p1_B4_C0_391	OR105528
PWH5_L2p1_A10_C0_341	OR105529
PWH3_L1p3_B11_C0_402	OR105530
PWH3_L1p3_A5_C0_417	OR105531
PWH3_L1p3_A3_C0_418	OR105532
PWH3_L1p2_H12_C0_390	OR105533
PWH3_L1p2_H4_C0_378	OR105534
PWH3_L1p2_G5_C0_392	OR105535
PWH3_L1p2_F2_C0_412	OR105536
PWH3_L1p2_D12_C0_394	OR105537
PWH3_L1p2_D3_C0_399	OR105538
PWH3_L1p2_C11_C0_329	OR105539
PWH3_L1p2_C8_C0_432	OR105540
PWH3_L1p2_C2_C0_366	OR105541
PWH3_L1p2_B10_C0_371	OR105542
PWH3_L1p2_A10_C0_42	OR105543
PWH3_L1p1_H7_C0_263	OR105544
PWH3_L1p1_G3_C0_365_inversion	OR105545
PWH3_L1p1_G1_C0_430	OR105546
PWH3_L1p1_F7_C0_350	OR105547
PWH3_L1p1_F3_C0_418_inversion	OR105548
PWH3_L1p1_E12_C0_413	OR105549
PWH3_L1p1_E10_C0_430	OR105550
PWH3_L1p1_D9_C0_436	OR105551
PWH3_L1p1_D8_C0_366	OR105552
PWH3_L1p1_C6_C0_390	OR105553
PWH3_L1p1_B5_C0_422	OR105554
PWH3_L1p1_B4_C0_392	OR105555
PWH3_L1p1_A6_C0_433	OR105556